JOURNAL OF MATERIALS SCIENCE **37** (2002) 2359–2365

Effect of heat treatment on phase stability, microstructure, and thermal conductivity of plasma-sprayed YSZ

R. W. TRICE*, Y. JENNIFER SU†, J. R. MAWDSLEY‡, K. T. FABER
Department of Materials Science and Engineering, Robert R. McCormick School of Engineering and Applied Science, Northwestern University, Evanston, Illinois 60208, USA
E-mail: k-faber@northwestern.edu

A. R. DE ARELLANO-LÓPEZ
Departamento de Física de la Materia Condensada, Universidad de Sevilla, Seville, Spain

HSIN WANG, W. D. PORTER
High Temperature Materials Laboratory, Oak Ridge National Laboratory, Oak Ridge, TN 37831, USA

The effects of 50-hour heat treatments at 1000°C, 1200°C, and 1400°C on air plasma-sprayed coatings of 7 wt% Y_2O_3-ZrO_2 (YSZ) have been investigated. Changes in the phase stability and microstructure were investigated using x-ray diffraction and transmission electron microscopy, respectively. Changes in the thermal conductivity of the coating that occurred during heat treatment were interpreted with respect to microstructural evolution. A metastable tetragonal zirconia phase, with a non-equilibrium amount of Y_2O_3 stabilizer, was the predominant phase in the as-sprayed coating. Upon heating to 1000°C for 50 hours, the concentration of the Y_2O_3 in the *t*-zirconia began to decrease as predicted by the Y_2O_3-ZrO_2 phase diagram. The *c*-ZrO_2 phase was first observed after the 50-hour heat treatment at 1200°C; monoclinic zirconia was observed after the 50-hour heat treatment at 1400°C. TEM analysis revealed closure of intralamellar microcracks after the 50-hour/1000°C heat treatment; however, the lamellar morphology was retained. After the 50-hour/1200°C heat treatment, a distinct change was observed in the interlamellar pores; equiaxed grains replaced the long, columnar grains, with some remnant lamellae still observed. No lamellae were observed after the 50-hour/1400°C heat treatment. Rather, the microstructure was equivalent when viewed in either plan view or cross-section, revealing large grains with regions of monoclinic zirconia. Thermal conductivity increased after every heat treatment. It is believed that changes in the intralamellar microcracks and/or interlamellar pores are responsible for the increase in thermal conductivity after the 1000°C and 1200°C heat treatments. The increase in thermal conductivity that occurs after the 50-hour/1400°C heat treatment is proposed to be due to the formation of *m*-ZrO_2, which has a higher thermal conductivity than tetragonal or cubic zirconia.

1. Introduction

Air plasma sprayed thermal barrier coatings (TBCs) offer improved operating efficiency for gas turbines used in land-based and aircraft-based applications by either increasing the operating temperature or decreasing the need for cooling of the metallic structure. For example, a 200 μm thick coating of 7 wt% Y_2O_3-stabilized ZrO_2 can lower the surface temperature of the metallic structure by 200°C [1]. Typical service temperatures range from 800°C to 1300°C for these coatings. However, both the microstructure and phase composition of these coatings are dynamic during service.

It is well established that during plasma spraying the molten YSZ undergoes rapid cooling upon impact with the substrate, forming a yttria-rich, non-equilibrium phase [2, 3]. Upon heating, the excess yttria slowly diffuses out of the metastable zirconia phase, ultimately leaving a tetragonal zirconia phase with an equilibrium amount of the stabilizer (approximately 4 wt% Y_2O_3). This equilibrium *t*-ZrO_2 phase will readily form

Present Address: Purdue University, School of Materials Engineering, West Lafayette, IN 47907, USA.
†*Present Address*: General Electric Co., Corporate Research and Development, Schenectady, NY 12309, USA.
‡*Present Address*: Argonne National Laboratory, Argonne, IL 60439, USA.

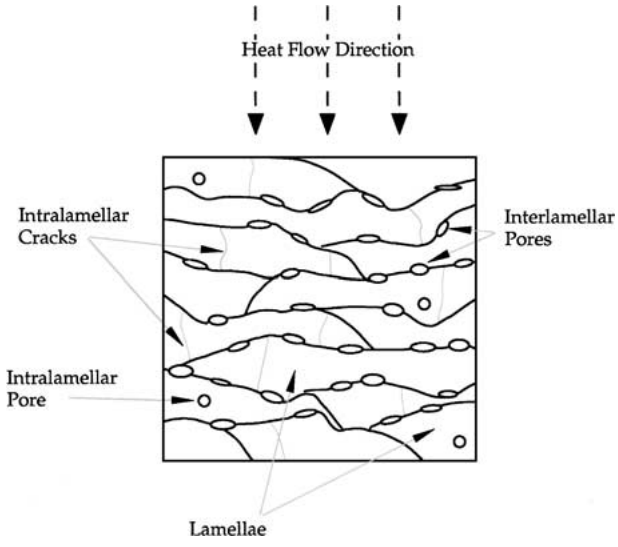

Figure 1 Schematic of the plasma-sprayed microstructure with dominant microstructural defects indicated.

m-ZrO_2 upon cooling. It is not uncommon to observe m-ZrO_2 after only a 10-hour heat treatment at 1400°C [4]. The excess yttria that originated in the metastable zirconia phase is used to nucleate and grow grains of c-ZrO_2, a zirconia phase with an equilibrium concentration of yttria of 14 wt%.

The as-sprayed microstructure is extremely complex, as shown schematically in Fig. 1. Small oblate pores (<0.1 μm) exist between the flattened powders or lamellae (i.e. interlamellar pores); the actual contact between adjacent lamellae has been suggested to be as low as 20% [5]. In addition, microcracks that span the thickness of the lamellae (intralamellar microcracks) are oriented approximately parallel with the spray direction. Intralamellar pores also exist. As temperature is increased, the microstructure tends to sinter within the range of the expected operating temperatures. Ilavsky *et al.* [6] have shown an overall reduction in the specific surface area of both the intralamellar microcracks and interlamellar pores as a function of heat treatment. The intralamellar microcracks are the first to close, beginning around 800°C. The reduction in the specific surface area of the microcracks levels off at approximately 1000°C. A reduction in the specific surface area associated with the interlamellar pores begins at ≈1100°C.

Both the phase transformation and the sintering effects increase the thermal conductivity. The transformation to m-ZrO_2 is undesirable because its intrinsic thermal conductivity is greater than that of the tetragonal phase [7]. Closure of the interlamellar pores and intralamellar cracks increases the efficiency through which heat is transferred through the coating [8], making the coating less insulative. Some prior research has been performed to investigate the effect of heat treatment on PS YSZ [9–11]. Dinwiddie *et al.* [9] focused on comparing the thermal conductivity of both EB-PVD and PS YSZ after heat treatments, with no phase analysis or microscopy performed. Mogro–Campero [10] looked at the effect of 1200°C and 1300°C heat treatments on thermal conductivity of PS YSZ using Larson–Miller fitting parameters to describe thermal conductivity aging effects. Eaton *et al.* [11] measured the change in thermal conductivity over a broad range of heat treatments (870°C–1400°C) using scanning electron microscopy to view microstructural changes. However, none of the studies monitored the formation of the monoclinic zirconia or viewed the heat-treated microstructures using TEM. In the research being reported presently, we combine transmission electron microscopy with X-ray diffraction techniques to correlate the microstructural changes that occur upon heating with the observed increase in thermal conductivity. Thus, we have investigated the effects of 50-hour heat treatments at 1000°C, 1200°C, or 1400°C on the phase stability and microstructure of stand-alone plasma-sprayed YSZ coatings. X-ray diffraction was used to determine the zirconia phases present and transmission electron microscopy was employed to discern changes in the lamellar and grain structure. The microstructural changes were interpreted with respect to the thermal conductivity of the coatings.

2. Experimental procedures

2.1. Plasma-spray process

A fused and crushed 7 wt% Y_2O_3-ZrO_2 powder[§] (YSZ), nominally 12 μm in diameter, was used in the current study. All coatings were sprayed using the small-particle plasma spray (SPPS) process at Northwestern University [12]. An A-3000 Plasma Technik control system with an F4 gun, mounted on a seven–axis ASEA Brown and Boveri IRB 2000 robot, was used to spray the coatings.

Each powder was fed into the plasma flame through an externally mounted SPPS injector using a standard disc feeder. The disc speed feeding the YSZ powder was held at a constant speed (3.5 relative units). The argon carrier gas that fed the YSZ was held constant at 9 standard liters per minute (slm), respectively. A 25 kW power setting with a primary plasma gas of Ar (at 45 slm) and secondary gas of H_2 (at 5 slm) was used. The spray distance, measured from the injector to the substrate, was 6 cm. The injector was placed 11 mm from the centerline of the flame. Cooling air was blown on the front and back of the substrates. The rastering speed of the torch across the substrates was 350 mm/s with a 3 mm drop between passes.

All coatings were sprayed on 1018 steel substrates that were initially plasma-spray coated with aluminum. The Al layer facilitated removal of the coating, as a weak HCl solution will preferentially attack the aluminum, separating the coating from the substrate. A 220-grit alumina powder was used to gritblast the polished aluminum coating prior to application of the ceramic coatings.

Stand-alone as-sprayed coatings were subjected to one of three different heat treatments of 50 hours duration. These included soak temperatures of 1000°C, 1200°C, and 1400°C. Thus, comparisons will be made of coatings in the as-sprayed condition and after 50 hours at 1000°C, 1200°C, or 1400°C.

[§]Amperit 825.0, H.C. Starck, Newton, MA, USA.

2.2. Physical property measurements and TEM foil preparation

The bulk density of the coatings, necessary to determine the thermal conductivity, was measured using the immersion technique. X-ray diffraction measurements, using Cu-K_α radiation, were made on stand-alone coatings of as-sprayed and heat treated YSZ using a Scintag Diffractometer (XDS 2000) to qualitatively determine the phases present using the method described by Muraleedharan *et al.* [13].

Plan view and cross-sections of the as-sprayed and heat treated YSZ coatings were thinned by wedge polishing[¶], followed by precision ion polishing[**] for about an hour, thinning both sides simultaneously. The samples were mounted to a copper grid between the two thinning processes. They were viewed in a Hitachi HF2000 cFEG.

2.3. Thermal conductivity measurements

A detailed description of the laser flash technique used to determine thermal diffusivity has been published previously [14]. All measurements were made at the High Temperature Materials Laboratory at Oak Ridge National Laboratory. A disk-shaped sample, 12.5 mm in diameter with a thickness varying from 160 to 500 μm, was used for all tests. Thermal diffusivity was measured between 25°C and 1200°C. The time-temperature curves were analyzed by the method of Clark and Taylor [15], which takes into account radiation losses and uses the heating part of the curve to calculate thermal diffusivity. The samples were tested in argon in two furnaces, one for measurements from 25°C through 500°C, and another for measurements from 600°C through 1200°C. The IR detector was also changed from an InSb detector to a Si detector between 500°C and 600°C. Three measurements were taken for each sample at each temperature and averaged. Samples were tested in sets of up to six; thermal conductivity measurements at each temperature took about 20–30 minutes for a complete set of six samples.

The specific heat was determined from 100°C through 1050°C for each coating with a differential scanning calorimeter[††] using sapphire as the reference standard. The heat-up rate was 20°C/min in an argon atmosphere. Samples were composed of 4 mm disks, stacked to achieve a mass of approximately 90 mg. The as-sprayed samples exhibited an exothermic peak in heat flow near 900°C. As a result, these samples were given a 1-hour heat treatment through 1000°C prior to testing.

Thermal conductivity of the coating at each temperature was calculated using $k = 100\alpha c_p \rho$ where α is the thermal diffusivity in cm^2/s, c_p is the specific heat in J/g-°C, and ρ is the density in g/cm^3. Specific heat values at 1100°C and 1200°C were estimated from a best-fit line to the data collected from 100°C through 1050°C. Density was assumed to be constant for the current measurements. The total error associated with each thermal conductivity value is ±6%.

[¶]South Bay Technology, San Clemente, CA, USA.
[**]Gatan, Model # 691.
[††]Omnitherm DSC 1500.

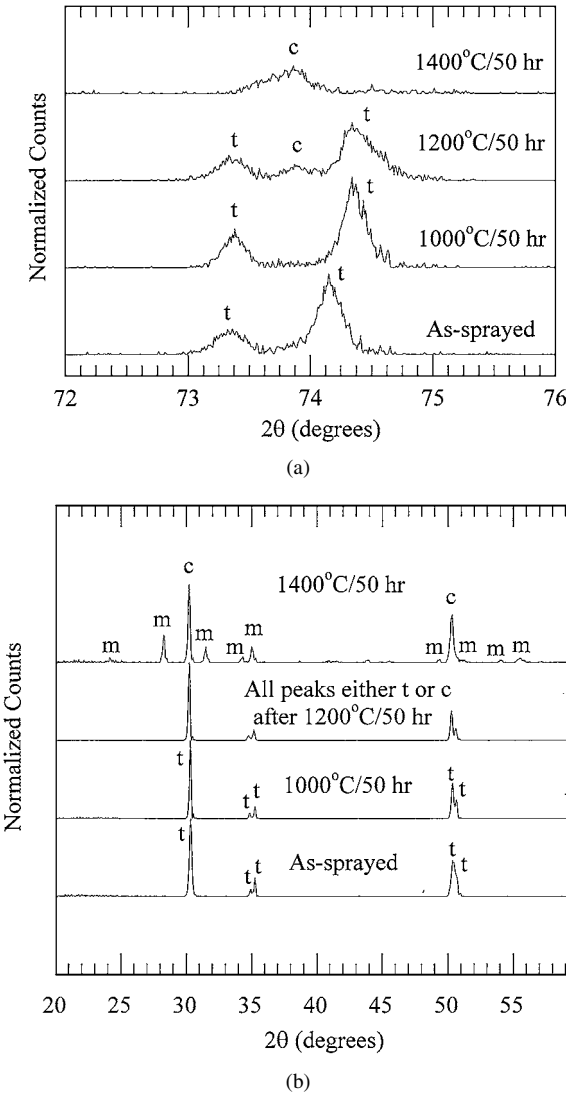

Figure 2 X-ray plots for the as-sprayed and heat treated coatings of YSZ between (a) 72–76° and (b) 20–60° ($t = t$-ZrO_2, $c = c$-ZrO_2, $m = m$-ZrO_2). As described in the text, the shift observed in plot a between the t-ZrO_2 peaks in the as-sprayed condition and after the 50 hr/1000°C heat treatment is due to a decrease in Y_2O_3 concentration in the tetragonal lattice.

3. Results and discussion

3.1. Phase stability

X-ray diffraction plots for the as-sprayed and heat treated samples of YSZ are shown in Fig. 2a and b. Plotting the x-ray diffraction results from 72–76° (see Fig. 2a) makes it possible to discriminate tetragonal zirconia phases with different amounts of Y_2O_3, and to differentiate between tetragonal and cubic zirconia phases. The x-ray diffraction results plotted from 20–60° more clearly show the development of m-ZrO_2.

The as-sprayed coating often contains a tetragonal phase with the same yttria concentration as the starting powder due to the high quench rates that occur during interaction of the melted particles with the substrate. This is a metastable tetragonal phase because it contains a non-equilibrium amount of yttria (7 wt%), whereas the Y_2O_3-ZrO_2 phase diagram would predict the t-ZrO_2 phase to contain 4 wt% yttria [3, 13]. The increased concentration of Y^{3+} ions in 7 wt% Y_2O_3-ZrO_2, which are 22% larger than Zr^{4+} ions, means that the unit cell is expanded as compared to the 4 wt%Y_2O_3-ZrO_2 phase, shifting diffraction peaks to smaller 2θ angles. This is

evident in the as-sprayed data in Fig. 2a, where the (400) peak for this non-equilibrium phase of zirconia occurs at 74.15°; for 4 wt%Y_2O_3-ZrO_2 the (400) peak is expected at 74.40°.

Upon heating, yttria diffuses out of the metastable zirconia phase until it reaches its equilibrium concentration of yttria as determined by the phase diagram (which is a function of the heat treatment temperature). Looking again at Fig. 2a, it is apparent that this phenomenon is occurring. For example, after 50 hours at 1000°C, the diffraction peak for the (400) plane has shifted to 74.40°, indicating that the concentration of Y^{3+} ions has decreased.

The yttria that has diffused out of the tetragonal zirconia resides in a newly formed c-ZrO_2 phase, with approximately 14 wt% Y_2O_3. As is the case with the t-ZrO_2 phase, the exact composition of the c-ZrO_2 phase is a function of the heat treatment temperature and can be reasonably determined from the phase diagram. It is not until after the 50 hr/1200°C heat treatment that a c-ZrO_2 peak appears, consistent with the slow diffusion of yttria from the metastable zirconia phase and the nucleation of cubic zirconia grains.

After the 1400°C heat treatment only the c-ZrO_2 peak is apparent in the 72–76° region of Fig. 2a. Fig. 2b further indicates that the coating has completely transformed to m-ZrO_2 and c-ZrO_2. Monoclinic zirconia forms upon cooling from the transformation of the equilibrium yttria concentration of t-ZrO_2, and is typically associated with a 3.5 vol% expansion [16].

3.2. Microstructural stability

TEM micrographs of cross-sectional and plan view-oriented samples in the as-sprayed and heat treated conditions are presented in Fig. 3. As expected, the cross-sectionally oriented sample in the as-sprayed condition (Fig. 3a) revealed the lamellar morphology, with each lamella comprised of columnar grains and submicron porosity between adjacent lamellae (interlamellar pores). Intralamellar porosity was also observed, but is not shown in the micrograph presented. Intralamellar microcracks were most apparent in the plan view orientation (Fig. 3b). Columnar grains from 50–200 nm in diameter to 0.5–2 μm long comprised the individual lamellae that made up the coatings.

Fig. 3c and d show the microstructure of a sample that has been heat treated for 50 hours at 1000°C in cross-sectional and plan view orientations, respectively. The long, columnar grains and lamellar morphology are

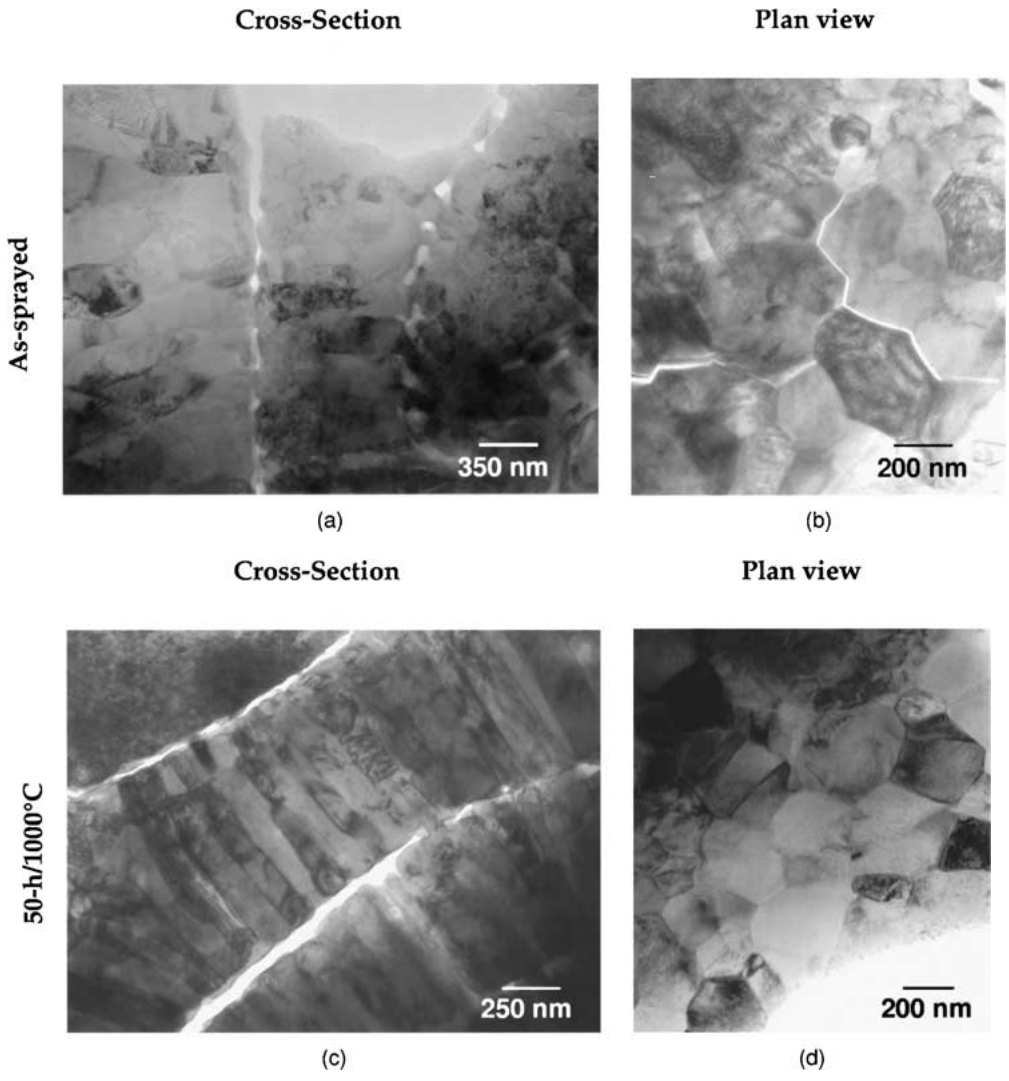

Figure 3 Bright field TEM micrographs of cross-sectional and plan view oriented samples in the as-sprayed and heat treated conditions: (a) as-sprayed cross-section (b) as-sprayed plan view (c) 50-h/1000°C cross-section (d) 50-h/1000°C plan view (e) 50-h/1200°C cross-section (f) 50-h/1200°C plan view (g) 50-h/1400°C cross-section (h) 50-h/1400°C plan view. (*Continued.*)

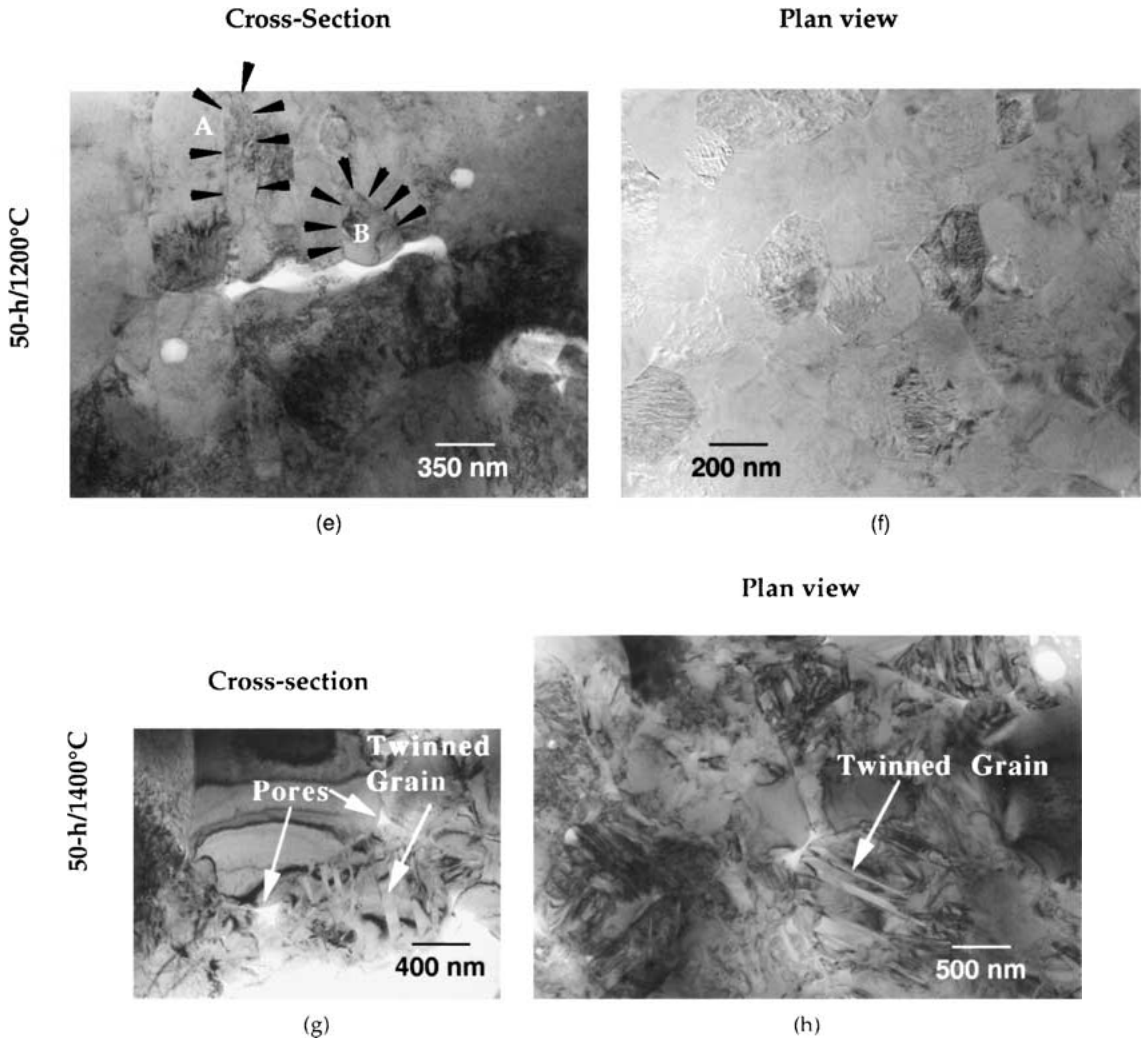

Figure 3 (*Continued.*)

still predominant in cross-section. However, gone are the microcracks that were observed in the as-sprayed condition (Fig. 3b). While it is difficult to qualitatively assess the intralamellar crack density using TEM, small angle neutron scattering has shown that intralamellar cracks heal after heat treatments at 1000°C [6].

Fig. 3e and f show a coating subjected for 50 hours at 1200°C in cross-sectional and plan view orientations, respectively. From Fig. 3e, some elongated grains still exist (see grain A) that are likely the tetragonal zirconia phase. In other regions, for example grain B, we observed equiaxed grains. Because X-ray results after the 1200°C treatment indicate that *c*-ZrO_2 (Fig. 2a) is forming, these non-columnar grains are likely *c*-ZrO_2. The lamellar morphology has been largely eliminated by the changes in the grain shape, but there were a few regions of the sample where remnant lamellae were noted. Fig. 3f reveals grains similar in size to those observed in the as-sprayed condition and the 50-hour/1000°C heat treatment.

The changes in the microstructure that occur after 50 hours at 1400°C are reported in Fig. 3g and h. Similar grain morphology is observed independent of orientation. The overall grain size has increased, most apparent in the plan view orientation (Fig. 3h). The grains are rounded (as opposed to hexagonal) with porosity located at the triple points of grain clusters. Both Fig. 3g and h reveal a *m*-ZrO_2 grain with twins.

3.3. Thermal conductivity

The thermal conductivity of plasma-sprayed Y_2O_3-ZrO_2 coatings is reduced compared to that of sintered, bulk Y_2O_3-ZrO_2 by the various defects in the microstructure resulting from the application process. The most significant in reducing thermal conductivity will be the porosity and/or microcracks that are oriented perpendicular to the direction of heat flow through the coating, as schematically illustrated in Fig. 1 [17, 18]. Changes in the shape, distribution, or surface area of the defects that occur upon heating will influence the thermal conductivity.

The effect of the microstructural changes on thermal conductivity is evident in Fig. 4, a plot of the thermal conductivity of the coating (k) versus temperature of the as-sprayed YSZ coating before and after various heat treatments. Looking first at the as-sprayed material, it is apparent that microstructural changes are occurring during the test as k begins to increase at ≈800°C (as a reminder, the sample is at each testing temperature for 20–30 minutes). This is consistent with observations by Ilavsky *et al.* [6] that revealed a significant reduction

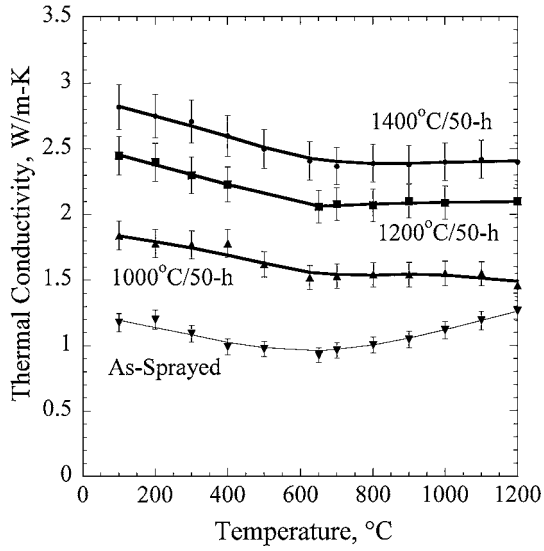

Figure 4 Plot of the thermal conductivity versus temperature for the as-sprayed condition and for various heat treatments.

in the specific surface area of the intralamellar cracks beginning near 800°C.

It is apparent in Fig. 4 that all three heat treatments increase the thermal conductivity, k, after each cycle. For example, at 700°C k varied from 1 W/m-K in the as-sprayed condition to 1.5, 2.1, and 2.4 W/m-K after 50-hour heat treatments at 1000°C, 1200°C, and 1400°C, respectively. At 1200°C k varied from 1.3 in the as-sprayed condition to 1.5, 2.1, and 2.4 W/m-K after 50-hour heat treatments at 1000°C, 1200°C, and 1400°C, respectively.

By interpreting the thermal conductivity data with respect to the TEM micrographs presented, some initial observations can be made on how microstructural changes affect thermal conductivity. It appears that closure or healing of the intralamellar microcracks are responsible for the increase in thermal conductivity at 1000°C. Though these microcracks are often modeled as perpendicular to the coating (and thus would not strongly influence the thermal conductivity), they are often shifted off normal. Furthermore, previous researchers have shown that the scatter in defect orientations from normal to the coating can have a pronounced effect on conductivity [18].

At 1200°C, the increase in thermal conductivity is likely due to the reduction in porosity as a result of sintering between the adjacent lamellae (Fig. 3e). A reduction in the specific surface area of the interlamellar pores of the coating has been observed to begin beyond 1000°C, with the most dramatic sintering effects observed beginning at 1100°C [6].

As shown in Fig. 2b, a significant fraction of the t-ZrO_2 begins to transform to m-ZrO_2 upon cooling as a result of the 50-hour/1400°C heat treatment. This transformation was also observed in the microstructure (see Fig. 3g). Estimates from previous researchers indicated that approximately 25 vol% m-ZrO_2 transforms upon cooling to room temperature after 50-hour at 1400°C [4]. For comparison, Table I lists the thermal conductivity of 98% dense m-ZrO_2, t-ZrO_2, and c-ZrO_2 at 200°C and 800°C [7]. The thermal conductivity of 98% dense m-ZrO_2 at 800°C was 3.6 W/m-K as compared to 2.8 W/m-K for similar density t-ZrO_2. Thus, transformation of tetragonal to monoclinic zirconia should result in an increase in k because a significant volume fraction of the coating is being replaced by a higher conductivity phase. This was observed in the current data as shown in Fig. 4.

TABLE I Thermal conductivity values of 98% dense m-ZrO_2, t-ZrO_2, and c-ZrO_2 as reproduced from [7]

Phase	k at 200°C (W/m-K)	k at 800°C (W/m-K)
m-ZrO_2	5.4	3.6
t-ZrO_2	2.8	2.8
c-ZrO_2	2.2	2.3

4. Conclusions

The effect of 50-hour heat treatments at 1000°C, 1200°C, and 1400° on air plasma-sprayed coatings of 7 wt% Y_2O_3-ZrO_2 (YSZ) has been investigated using x-ray diffraction and transmission electron microscopy. Coatings were initially composed of metastable zirconia phase with a non-equilibrium amount of yttria stabilizer. Upon heating, the yttria diffuses out of the metastable zirconia phase as predicted by the phase diagram, resulting in a tetragonal zirconia phase with an equilibrium concentration of stabilizer (approximately 4 wt% Y_2O_3). The excess yttria is used to nucleate and grow grains of c-ZrO_2 as a result of 50-hour holds at 1200°C and 1400°C. Monoclinic zirconia first appeared after the 50-hour hold at 1400°C. TEM revealed closure of intralamellar microcracks after the 50-hour/1000°C heat treatment; however, the lamellar morphology was retained. After the 50-hour/1200°C heat treatment, a reduction in the interlamellar pores was observed, with the long, columnar grains replaced by equiaxed grains and only a small fraction of the lamellar morphology retained. Only large equiaxed grains, with no lamellar morphology, were observed after the 50-hour/1400°C heat treatment.

The changes that occurred in thermal conductivity due to the heat treatment were interpreted with respect to the structural and microstructural changes observed with x-ray diffraction and TEM, respectively. It was proposed that several temperature dependent mechanisms that lead to an increase in the thermal conductivity of the coating are operative. The increase in k after 50 hours at 1000°C is likely due to closure of the intralamellar microcracks. The increase in k after 50 hours at 1200°C is proposed to be mainly due to sintering of the interlamellar porosity. After 50 hours at 1400°C, the increase in k is believed to be a result of the increasing volume fraction of high conductivity m-ZrO_2 in the coating.

Acknowledgments

The authors wish to thank Dr. Wen-An Chiou for assistance with the TEM. This work was supported by the U.S. Department of Energy, Federal Energy

Technology Center, Cooperative Agreement No. DE-FC21-92MC29061, under subcontract 96-01-SR047. A. R. de Arellano-López was supported by the Eschbach Visiting Scholar Program of the McCormick School of Engineering and Applied Science at Northwestern University. The thermal conductivity testing was supported by the U.S. DOE, Assistant Secretary for Energy Efficiency and Renewable Energy, Office of Transportation Technologies, as part of the HTML User Program under contract DE-AC05-00OR22725, managed by UT-Batelle, LLC.

References

1. R. A. MILLER, *Surf. Coat. Tech.* **30** (1987) 1.
2. L. LELAIT, S. ALPERINE, C. DIOT and M. MEVREL, *Mat. Sci. Eng.* A. **A121** (1989) 475.
3. V. LANTERI, R. CHAIM and A. H. HEUER, *J. Amer. Ceram. Soc.* **69**(10) (1986) C251.
4. J. ILAVSKY, J. WALLACE and J. K. STALICK, in Proceedings of the 1st International Thermal Spray Conference, May 2000, edited by C. C. Berndt (ASM International, Materials Park, OH) p. 1185.
5. R. MCPHERSON, *Surf. Coat. Tech.* **39/40** (1989) 173.
6. J. ILAVSKY, G. G. LONG, A. J. ALLEN and C. C. BERNDT, *Mat. Sci. Eng.* A. **A272** (1999) 215.
7. S. RAGHAVAN, H. WANG, R. B. DINWIDDIE, W. D. PORTER and M. J. MAYO, *Scripta Mater.* **38**(8) (1998) 1119.
8. R. DUTTON, R. WHEELER, K. S. RAVICHANDRAN and K. AN, *J. Therm. Spray* **9** (2000) 204.
9. R. B. DINWIDDIE, S. C. BEECHER, W. D. PORTER and B. A. NAGARAJ, in Proceedings of 41st Am. Soc. Mech. Eng. Int. Gas Turbine and Aeroengine, Birmingham, United Kingdom, June 1996.
10. A. MOGRO-CAMPERO, in "Thermal Conductivity 25," edited by C. Uher and D. Morelli (Technomic Publishing, Lancaster, PA, 1999) p. 183.
11. H. E. EATON, J. R. LINSEY and R. B. DINWIDDIE, in "Thermal Conductivity 22," edited by T. W. Tong (Technomic Publishing, Lancaster, PA, 1994) p. 289.
12. T. F. BERNECKI and D. R. MARRON, U.S. Patents Nos. 5,744,777 (1998) and 5,858,470 (1999).
13. K. MURALEEDHARAN, J. SUBRAHMANYAM and S. B. BHADURI, *J. Amer. Ceram. Soc.* **71**(5) (1988) C226.
14. H. WANG, R. B. DINWIDDIE and P. A. GAAL, in "Thermal Conductivity 23," edited by K. E. Wilkes, R. B. Dinwiddie and R. S. Graves (Technomic Publishing, Lancaster, PA, 1996) p. 119.
15. L. M. CLARK III and R. E. TAYLOR, *J. Appl. Phys.* **46**(2) (1975) 714.
16. A. H. HEUER, *J. Amer. Ceram. Soc.* **70**(10) (1987) 689.
17. R. MCPHERSON, *Thin Solid Films* **112** (1984) 89.
18. I. SEVOSTIANOV and M. KACHANOV, *Mat. Sci. Eng.* A. **297**(1-2) (2001) 235.

Received 15 January
and accepted 21 December 2001